Science Advances
AAAS

advances.sciencemag.org/cgi/content/full/6/6/eaay2669/DC1

Supplementary Materials for

Phosphoregulation of Rad51/Rad52 by CDK1 functions as a molecular switch for cell cycle–specific activation of homologous recombination

Gyubum Lim, Yeonji Chang, Won-Ki Huh*

*Corresponding author. Email: wkh@snu.ac.kr

Published 7 February 2020, *Sci. Adv.* **6**, eaay2669 (2020)
DOI: 10.1126/sciadv.aay2669

This PDF file includes:

Supplementary Figure Legends

Figure S1

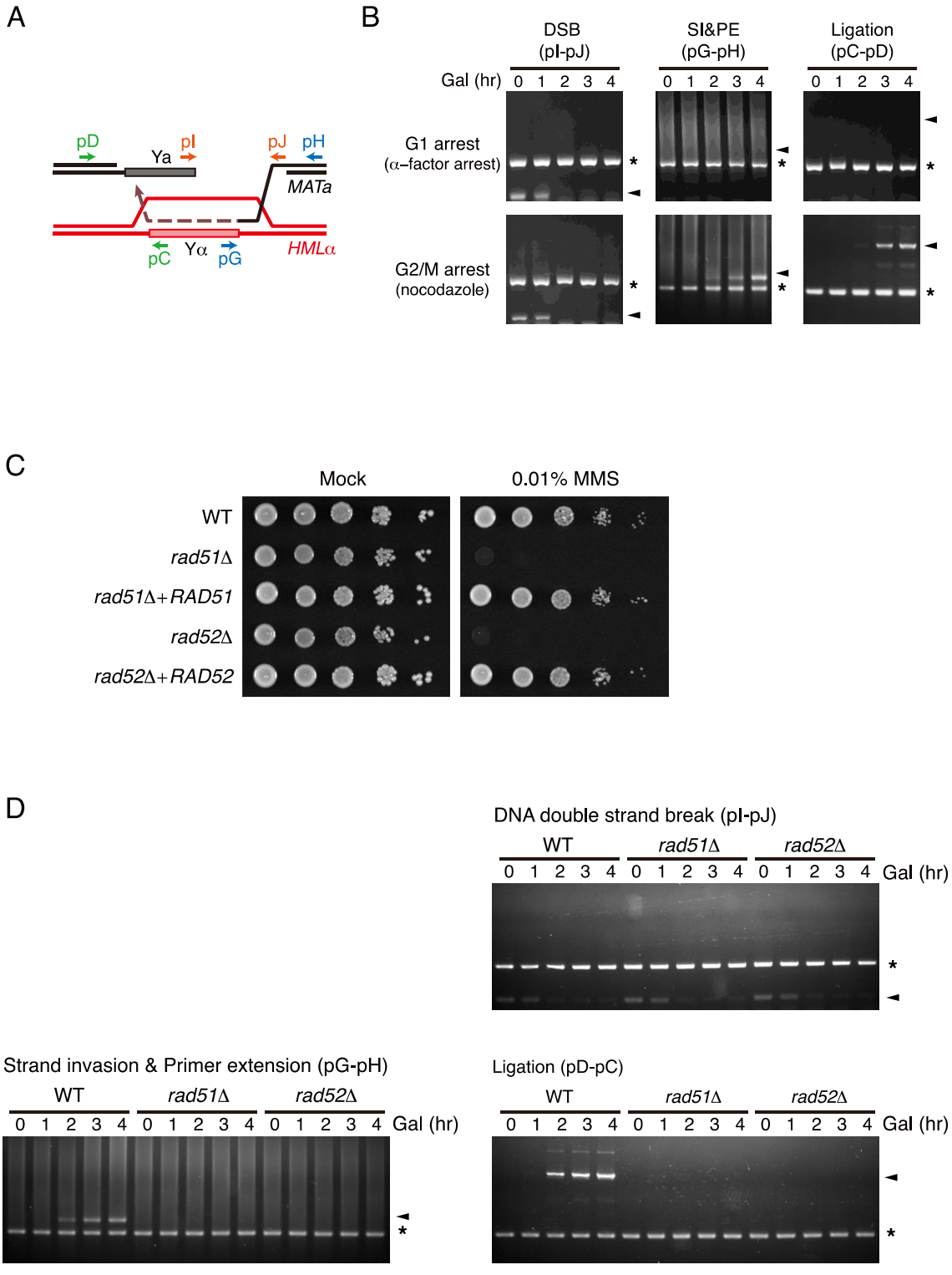

Fig. S1. Deletion of either *RAD51* or *RAD52* impairs DNA damage repair process. (**A**) The D-loop structure at the *MAT* locus with the binding positions of primers for PCR-based homologous recombination efficiency test. (**B**) Homologous recombination efficiency test in the G1- or G2/M-arrested cells. Cells were arrested for 3 hr with α-factor (150 μM) for G1 arrest and nocodazole (15 μg ml^{-1}) for G2/M arrest. Genomic DNA was extracted every 1 hr after 2% galactose addition and analyzed by PCR. SI&PE indicates strand invasion and primer extension. Arrowheads indicate the PCR products of the homologous recombination intermediates. Asterisks indicate the PCR products of the control region (*ARG5,6*). (**C**) Serial dilution assay used to assess MMS sensitivity of *rad51*Δ and *rad52*Δ cells. All strains were serially diluted on SC agar plates in the absence or presence of 0.01% MMS. (**D**) Homologous recombination efficiency test of *rad51*Δ and *rad52*Δ cells. Genomic DNA was extracted every 1 hr after 2% galactose addition and analyzed by PCR. Arrowheads indicate the PCR products of the homologous recombination intermediates. Asterisks indicate the PCR products of the control region (*ARG5,6*).

Figure S2

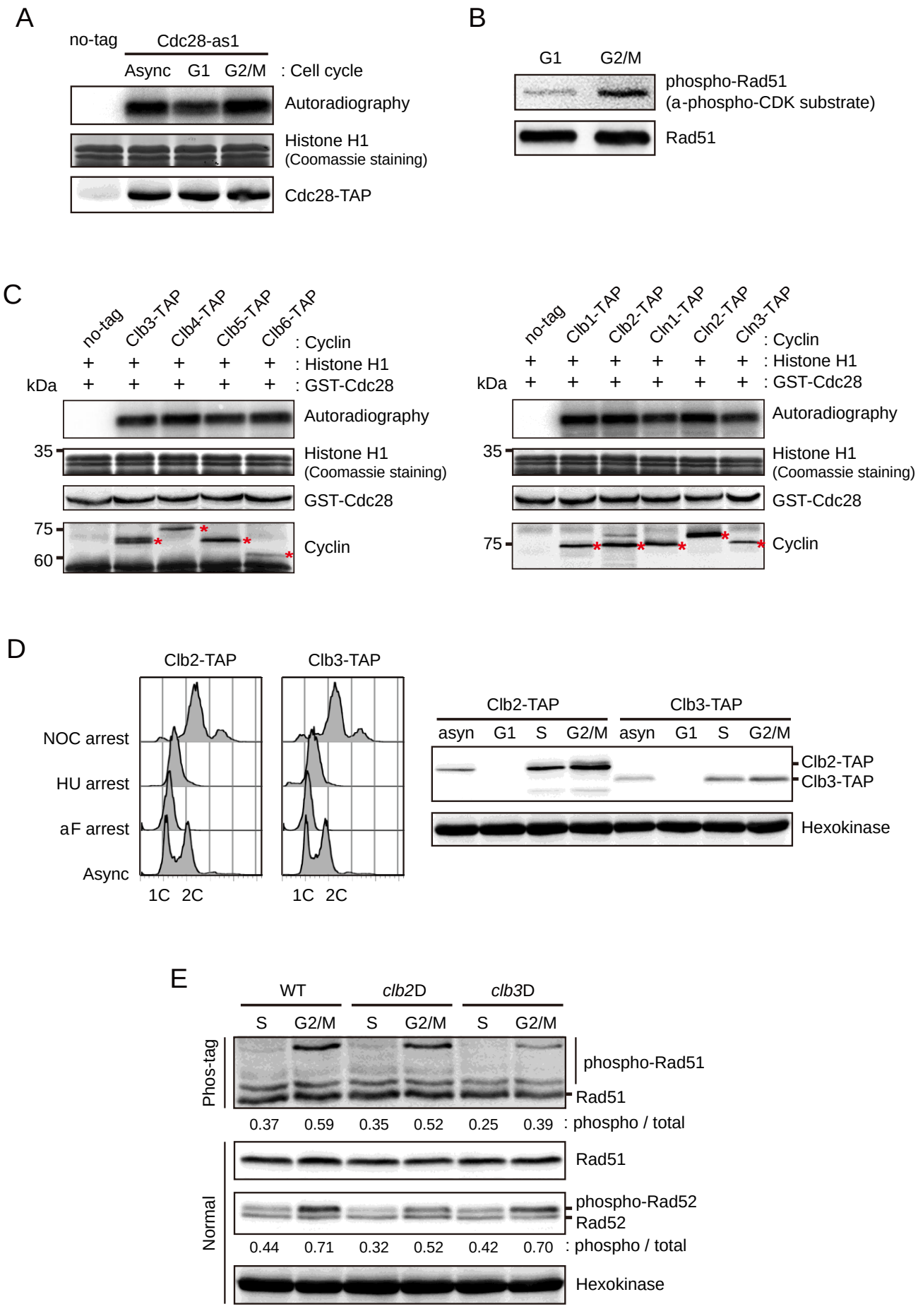
A
no-tag
Cdc28-as1
Async G1 G2/M : Cell cycle
Autoradiography
Histone H1
(Coomassie staining)
Cdc28-TAP
B
G1 G2/M
phospho-Rad51
(a-phospho-CDK substrate)
Rad51
C
no-tag Clb3-TAP Clb4-TAP Clb5-TAP Clb6-TAP
: Cyclin
: Histone H1
: GST-Cdc28
kDa
Autoradiography
35
Histone H1
(Coomassie staining)
GST-Cdc28
75
60
Cyclin
no-tag Clb1-TAP Clb2-TAP Cln1-TAP Cln2-TAP Cln3-TAP
D
Clb2-TAP
Clb3-TAP
NOC arrest
HU arrest
aF arrest
Async
1C 2C
asyn G1 S G2/M
Hexokinase
E
WT
clb2D
clb3D
S G2/M
Phos-tag
phospho-Rad51
Rad51
0.37 0.59 0.35 0.52 0.25 0.39 : phospho / total
Normal
phospho-Rad52
Rad52
0.44 0.71 0.32 0.52 0.42 0.70 : phospho / total

Fig. S2. Deletion of either *CLB2* or *CLB3* affects the phosphorylation of Rad51 and Rad52 in cells. (**A**) Results from the kinase assay for the phosphorylation of histone H1 using Cdc28 extracted from cell cycle-arrested cells in vitro. The cell cycle was arrested for 3 h with α-factor (150 μM) to arrest G1 and nocodazole (15 μg ml^{-1}) to arrest G2/M. (**B**) Identification of cell cycle-dependent phosphorylation of Rad51 by using the phospho-CDK substrate antibody. The cell cycle was arrested as described in (A). Rad51 proteins were immunoprecipitated by anit-HA beads, and analyzed by immunoblot assay. (**C**) Results from the kinase assay for the phosphorylation of histone H1 using purified Cdc28 and cyclins in vitro. Each cyclin was purified by anti-TAP immunoprecipitation from asynchronous cells. Red asterisks indicate bands of corresponding cyclins. (**D**) Analysis of the expression level of Clb2 and Clb3 through the cell cycle. The cell cycle was arrested for 3 h with α-factor (150 μM) to arrest G1, Hydroxyurea (200 mM) to arrest S, and nocodazole (15 μg ml^{-1}) to arrest G2/M. The DNA content data were analyzed by flow cytometry (left panel). 1C and 2C indicate single and double DNA haploid content, respectively. (**E**) Analysis of the in vivo phosphorylation level of Rad51 and Rad52 in *clb2*Δ or *clb3*Δ cells. The cell cycle was arrested as described in (D). 50 μM Phos-tag and 100 μM $MnCl_2$ were mixed with 6% separating gel for analysis of phospho-Rad51 (upper panel). The relative ratio of phosphorylated proteins to total proteins is shown below each lane.

Figure S3

A

Protein	Residue	Sequence	Kinase	Score	Cutoff
Rad51	S125	^{118} LLEIKGI**S**EAKADKL ^{132}	Cdc28	9.806	9.411
Rad51	S375	^{368} RLCKVVD**S**PCLPEAE ^{382}	Cdc28	11.833	9.411
Rad52	T412	^{406} QVPRET**T**PIKTNAT ^{419}	Cdc28	17.25	9.411

B

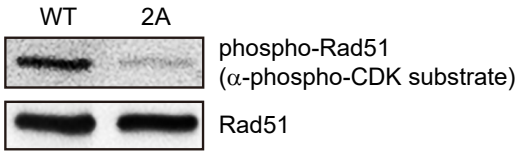

C

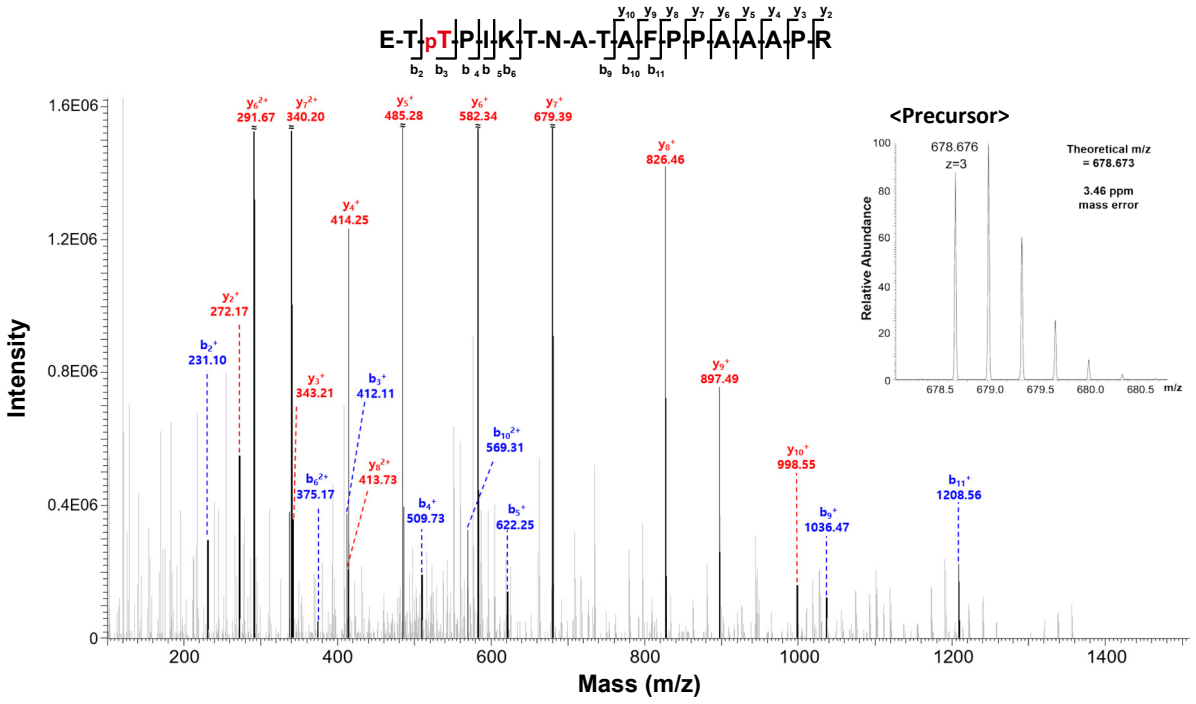

Fig. S3. CDK1 phosphorylates S125 and S375 of Rad51 and T412 of Rad52 in cells. (**A**) The prediction of Cdc28-dependent phosphorylated residues of Rad51 and Rad52 by GPS 3.0. S and T in red indicate serine and threonine residues that were predicted to be phosphorylated. (**B**) Identification of Cdc28-dependent phosphorylated residues of Rad51 by using the phospho-CDK substrate antibody. WT and 2A indicate wild-type Rad51 and Rad51-2A, respectively. Rad51 proteins were immunoprecipitated by anti-HA beads, and analyzed by immunoblot assay. (**C**) Identification of Cdc28-dependent phosphorylated residues of Rad52 by mass spectrometry.

Figure S4

G1 arrest (α–factor arrest)

DNA double strand break (pI-pJ)

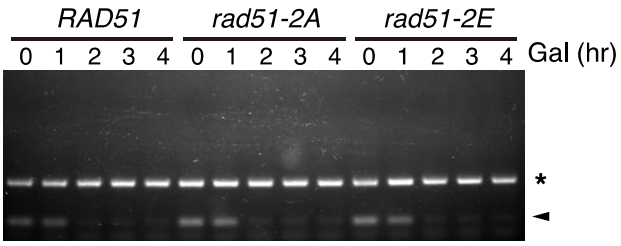

Strand invasion & Primer extension (pG-pH)

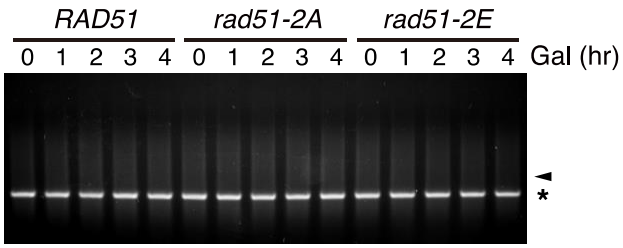

Ligation (pD-pC)

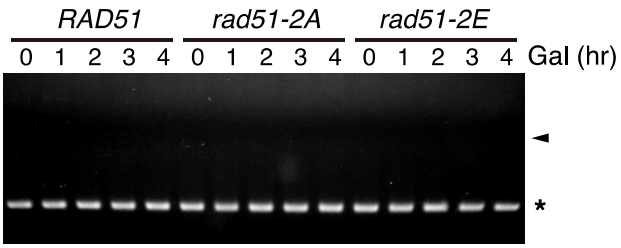

G2/M arrest (nocodazole)

DNA double strand break (pI-pJ)

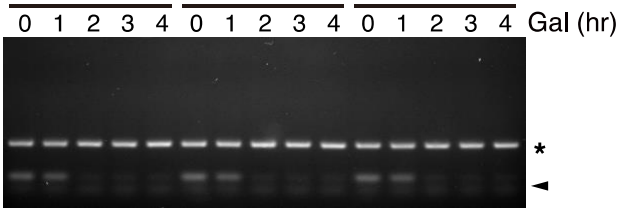

Strand invasion & Primer extension (pG-pH)

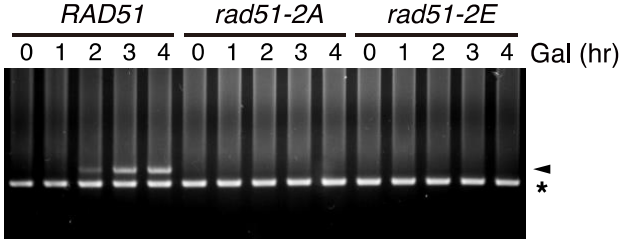

Ligation (pD-pC)

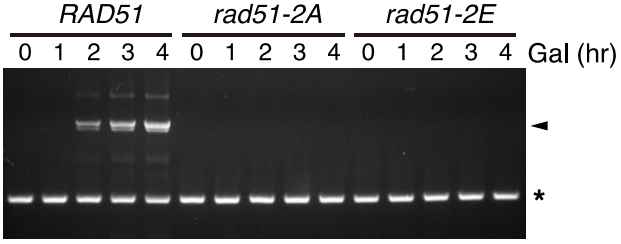

Fig. S4. Nonphosphorylatable mutation of Rad51 impairs the strand invasion process even in the G_2/M phase–arrested cells. Homologous recombination efficiency of *rad51-2A* cells was examined under cell cycle-arrested conditions. All strains were grown in YP media containing 2% raffinose to OD_{600} = 1.0 and diluted to OD_{600} = 0.5. 150 μM α-factor and 15 μg ml^{-1} nocodazole were treated to synchronize cell cycle to the G1 and G2/M phase, respectively. Genomic DNA was extracted every 1 hr after 2% galactose addition and analyzed by PCR. Arrowheads indicate the PCR products of the homologous recombination intermediates. Asterisks indicate the PCR products of the control region (*ARG5,6*).

Figure S5

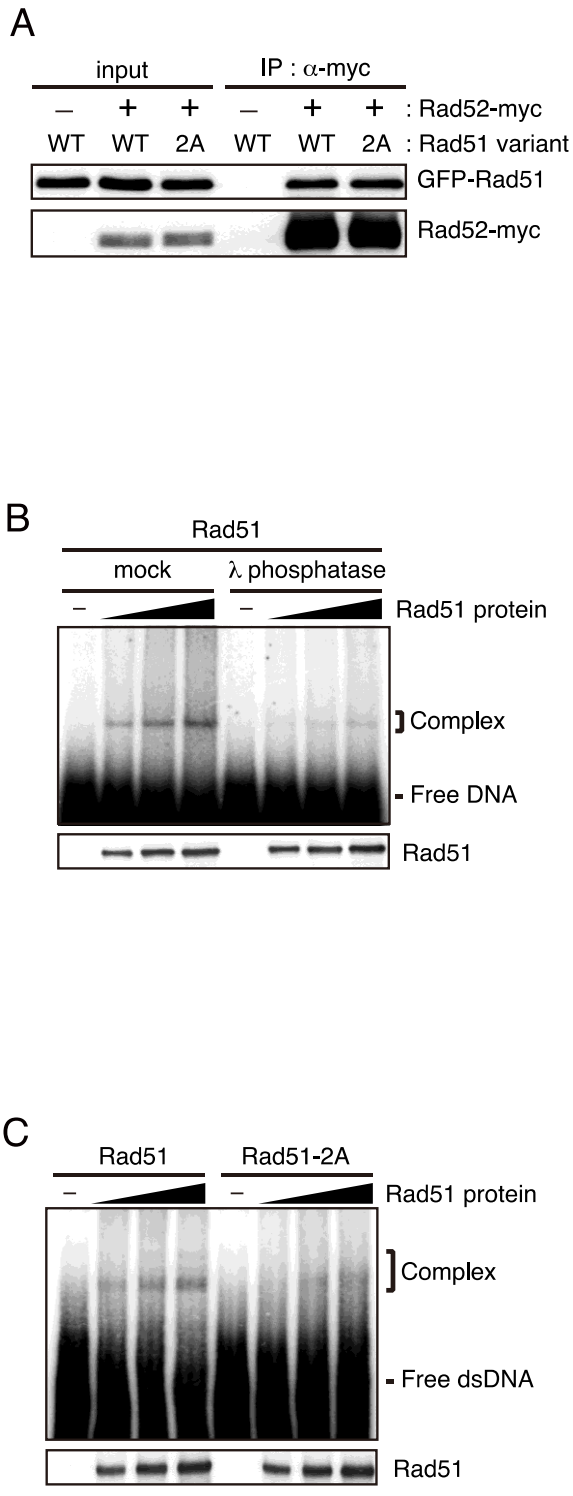
A
input
IP : α-myc
– + + – + + : Rad52-myc
WT WT 2A WT WT 2A : Rad51 variant
GFP-Rad51
Rad52-myc
B
Rad51
mock
λ phosphatase
– –
Rad51 protein
Complex
Free DNA
Rad51
C
Rad51
Rad51-2A
– –
Rad51 protein
Complex
Free dsDNA
Rad51

Fig. S5. CDK1-dependent phosphorylation regulates the DNA binding affinity of Rad51. (**A**) Coimmunoprecipitation assay used to assess the binding affinity between Rad52 and Rad51 variants. Protein complexes with Rad52-myc were precipitated using anti-myc antibody. Rad51 and Rad51-2A were detected by anti-GFP immunoblotting. (**B**) Results from the EMSA used to assess the effect of dephosphorylation on the ssDNA-binding affinity of Rad51. 800 units of λ phosphatase were directly added to Rad51 protein. EMSA was performed using a binding buffer that includes 35 mM Tris-Cl, pH 7.5, 5 mM ATP, 5 mM $MgCl_2$, 50 mM KCl, 100 μg/ml bovine serum albumin, and 1 mM dithiothreitol. (**C**) Results from the EMSA used to assess the dsDNA-binding affinity of Rad51 and Rad51-2A.

Figure S6

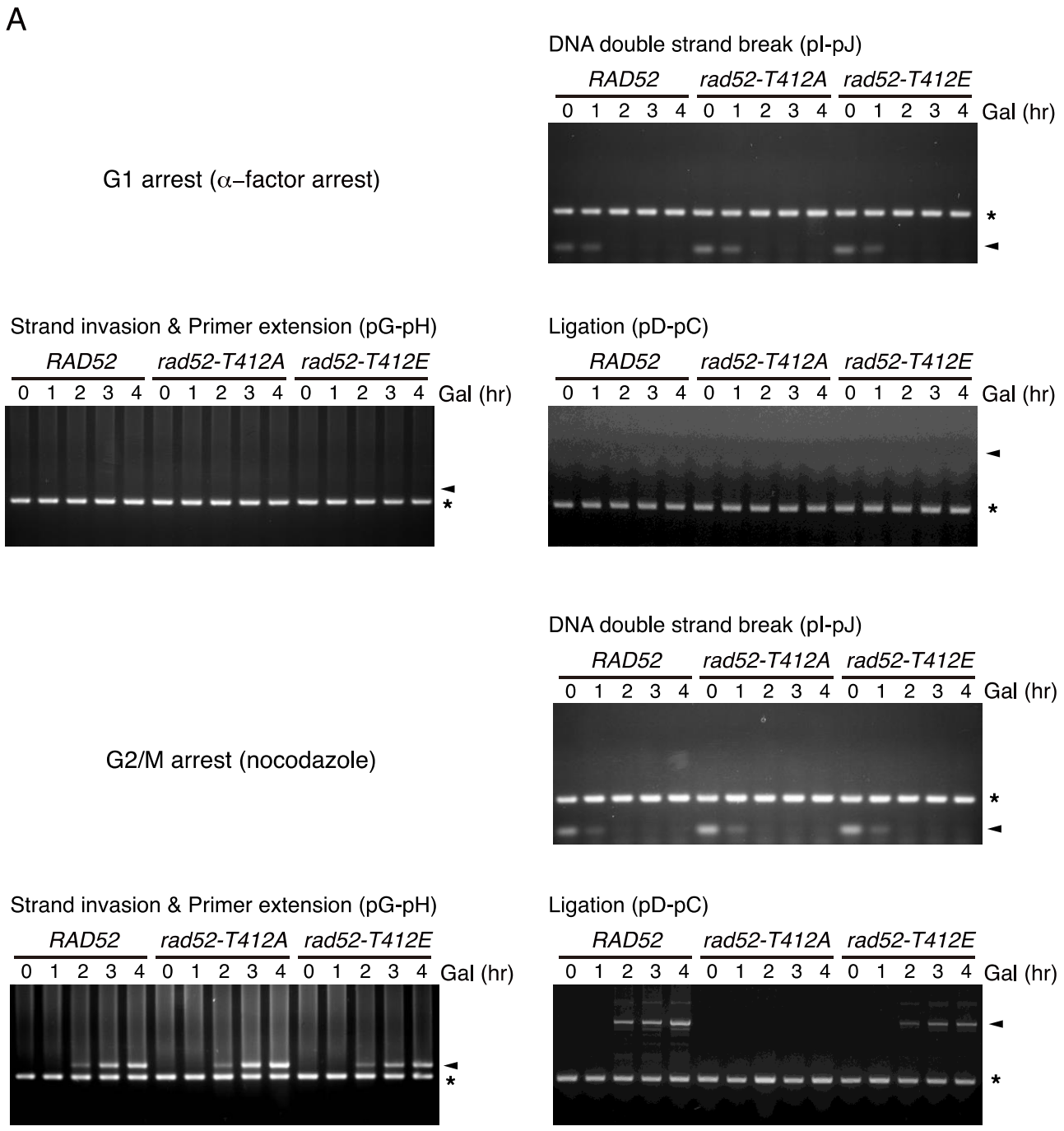
A
G1 arrest (α–factor arrest)
DNA double strand break (pI-pJ)
RAD52
rad52-T412A
rad52-T412E
0 1 2 3 4 0 1 2 3 4 0 1 2 3 4
Gal (hr)
Strand invasion & Primer extension (pG-pH)
Ligation (pD-pC)
G2/M arrest (nocodazole)
B
mock
λ phosphatase
WT T412A WT T412A : Rad52 variant
Rad52-HA
1 1.02 0.97 0.99 : relative Rad52 amount
Hexokinase

Fig. S6. Nonphosphorylatable mutation of Rad52 impairs ligation process even in the G_2/M phase–arrested cells. (**A**) Homologous recombination efficiency test of *rad52-T412A* cells under cell cycle-arrested conditions. Experiments were performed as described in fig. S1B (**B**) λ phosphatase treatment used to assess the protein amount of Rad52 and Rad52-T412A. 400 units of λ phosphatase were directly treated to each cell lysate. The relative amount of Rad52, normalized against that of wild-type Rad52 without λ phosphatase treatment, is shown below each lane. Hexokinase was used as a loading control.

Figure S7

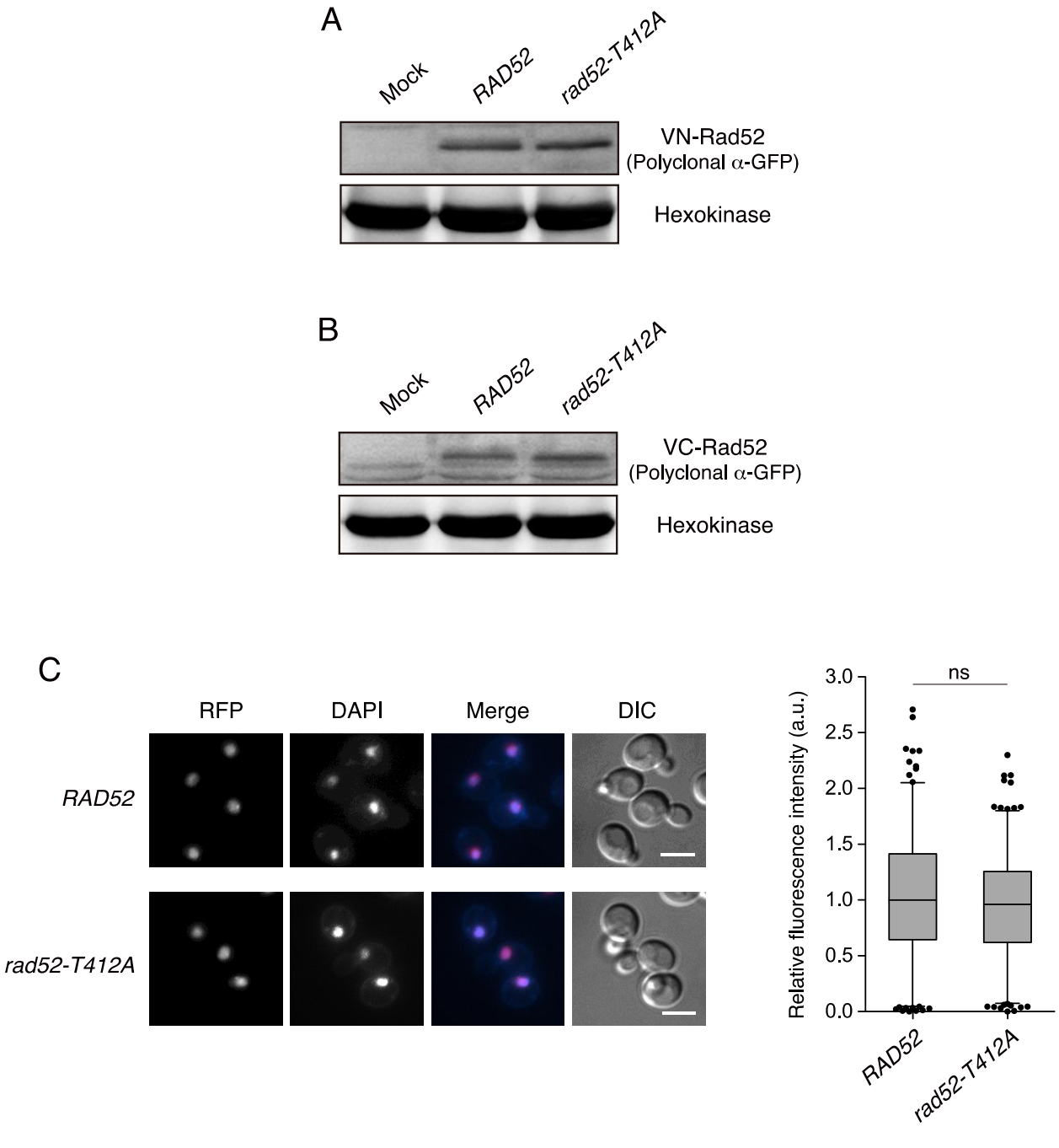
A
Mock
RAD52
rad52-T412A
VN-Rad52
(Polyclonal α-GFP)
Hexokinase
B
Mock
RAD52
rad52-T412A
VC-Rad52
(Polyclonal α-GFP)
Hexokinase
C
RFP
DAPI
Merge
DIC
RAD52
rad52-T412A
ns
Relative fluorescence intensity (a.u.)
3.0
2.5
2.0
1.5
1.0
0.5
0.0
RAD52
rad52-T412A
D
Rad52
Rad52-T412A

Fig. S7. Both wild-type Rad52 and Rad52-T412A form ring structures. (**A**) Western blot analysis used to assess the protein amount of VN-tagged Rad52 and Rad52-T412A. *RAD52* indicates the *MAT***a** cells expressing VN-Rad52 and *rad52-T412A* indicates the *MAT***a** cells expressing VN-Rad52-T412A. Immunoblotting for the detection of VN-tagged Rad52 was performed using the polyclonal anti-GFP antibody. Hexokinase was used as a loading control. (**B**) Western blot analysis used to assess the protein amount of VC-tagged Rad52 and Rad52-T412A. *RAD52* indicates the *MAT*α cells expressing VC-Rad52 and *rad52-T412A* indicates the *MAT*α cells expressing VC-Rad52-T412A. Immunoblotting for the detection of VC-tagged Rad52 was performed using the polyclonal anti-GFP antibody. Hexokinase was used as a loading control. (**C**) Comparison of the efficiency of nuclear transport of Rad52 and Rad52-T412A. *RAD52* and *rad52-T412A* indicate cells expressing Rad52-mCherry and Rad52-T412A-mCherry, respectively. Nuclei were visualized by 1 μg ml^{-1} DAPI staining (left panel). Scale bars are 4 μm. The fluorescence intensity was calculated by subtracting the background intensity from the RFP signal intensity (right panel). A box plot is represented with whiskers from the 5th to the 95th percentile, and the data were normalized to the median of *RAD52* cells (N > 200). *P*-values were determined by the Mann-Whitney *U* test (ns, not significant). (**D**) The protein complex of Rad52 and Rad52-T412A analyzed by transmission electron microscopy. Rad52 proteins were negatively stained by uranyl acetate. Scale bars are 10 nm.

Figure S8

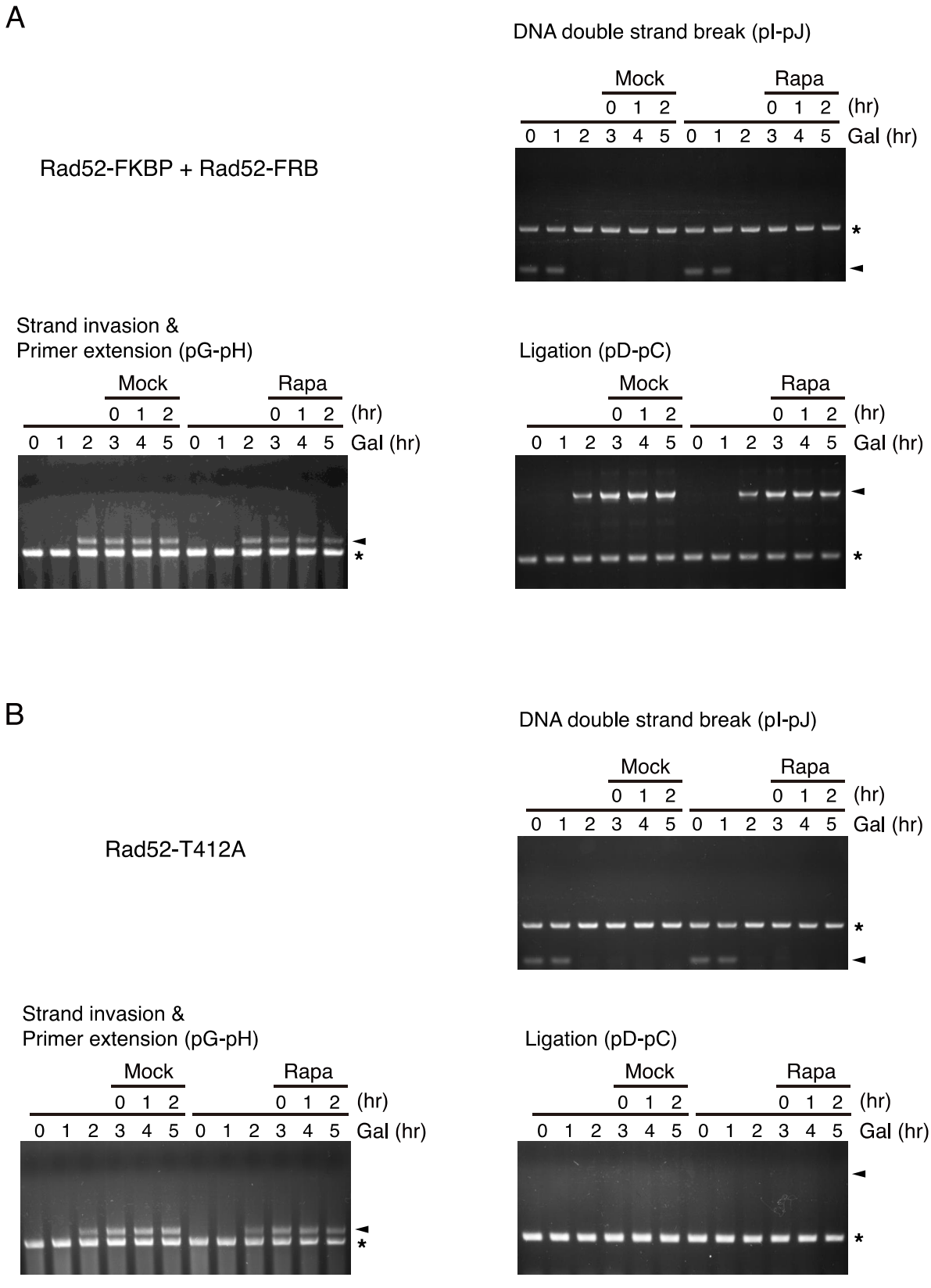
A
Rad52-FKBP + Rad52-FRB
DNA double strand break (pI-pJ)
Mock
Rapa
0 1 2 (hr)
0 1 2 3 4 5 0 1 2 3 4 5 Gal (hr)
*
Strand invasion &
Primer extension (pG-pH)
Ligation (pD-pC)
B
Rad52-T412A
DNA double strand break (pI-pJ)
Strand invasion &
Primer extension (pG-pH)
Ligation (pD-pC)

Fig. S8. Rapamycin treatment does not restore the defect in the ligation process in cells that express Rad52-T412A protein without FKBP or FRB attachment. (**A**) Homologous recombination efficiency test of cells expressing both wild-type Rad52 proteins attached to either FKBP or FRB. (**B**) Homologous recombination efficiency test of cells expressing Rad52-T412A protein without FKBP or FRB attachment. Genomic DNA was extracted every 1 hr after 2% galactose addition and analyzed by PCR. 1 μM rapamycin or DMSO was added to cell cultures at 3 hr after galactose addition. Arrowheads indicate the PCR products of the homologous recombination intermediates. Asterisks indicate the PCR products of the control region (*ARG5,6*).

Figure S9

For Figure 1A left

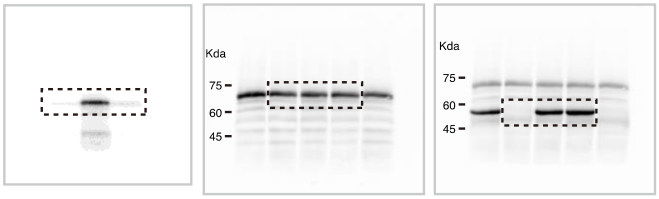

For Figure 1A right

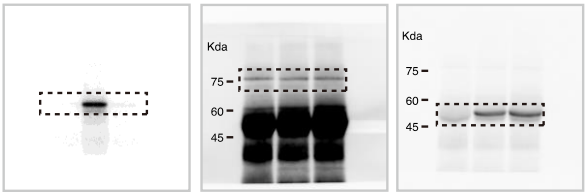

For Figure 1B left

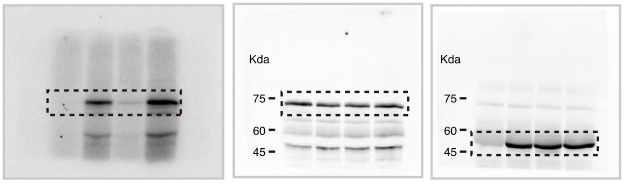

For Figure 1B right

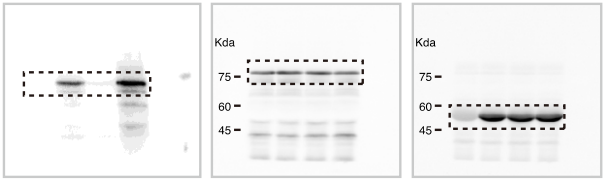

For Figure 1C

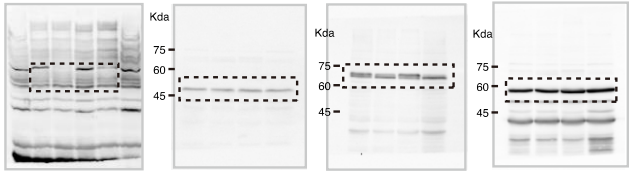

For Figure 2A left

For Figure 2A right

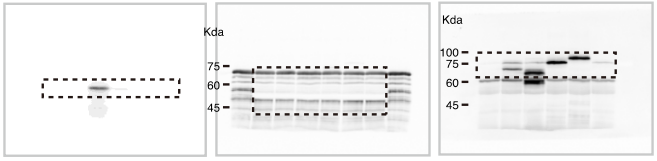

For Figure 2B left

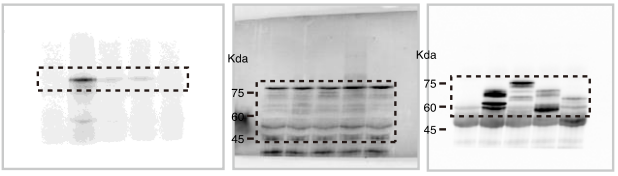

For Figure 2B right

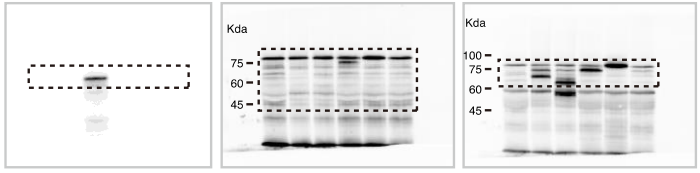

For Figure 2C

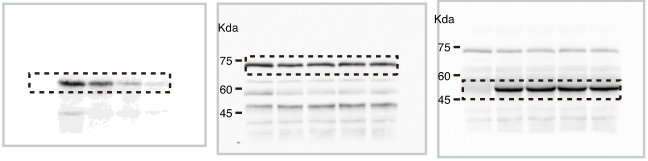

For Figure 2E

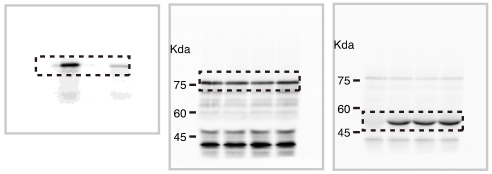

For Figure 3E

For Figure 3F

For Figure 4E

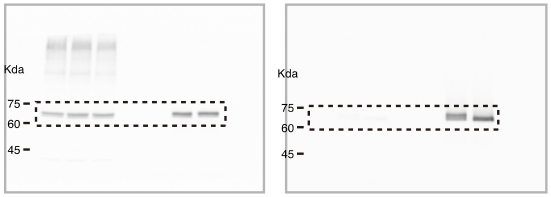

For Figure 4F

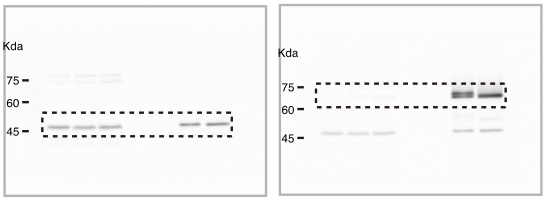

For Figure S2A

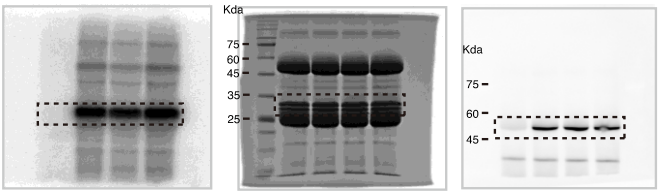

For Figure S2B

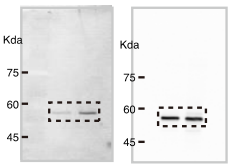

For Figure S2C left

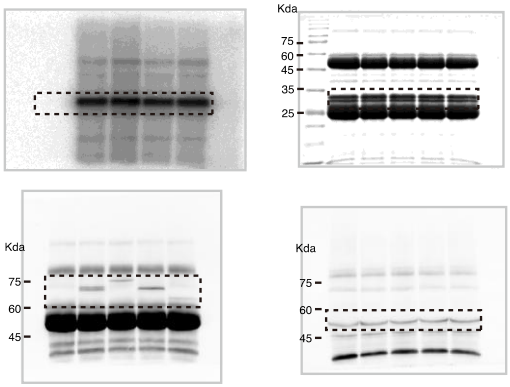

For Figure S2C right

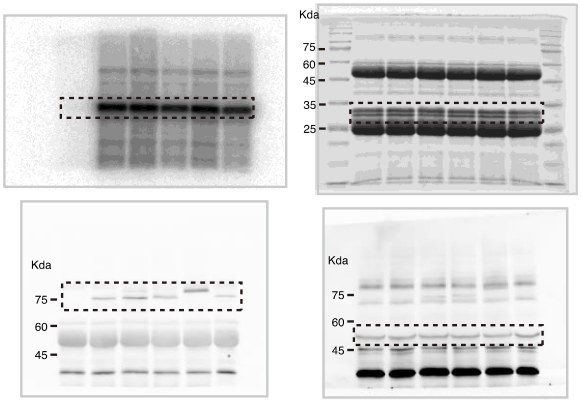

For Figure S2D

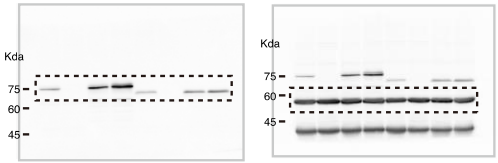

For Figure S2E

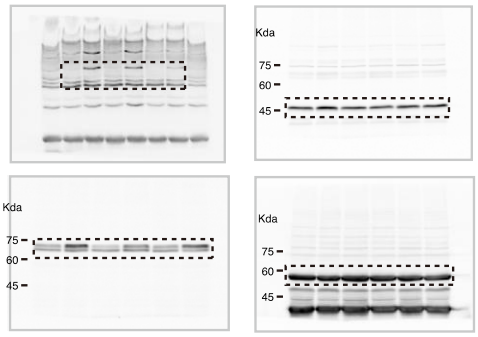

For Figure S3B

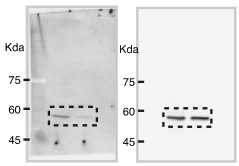

For Figure S5A

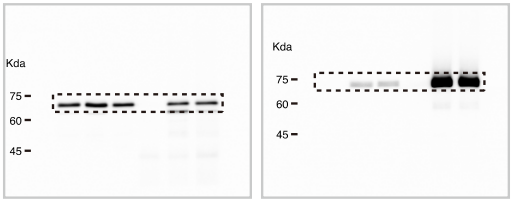

For Figure S5B

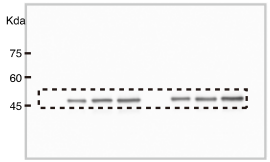

For Figure S5C

For Figure S6B

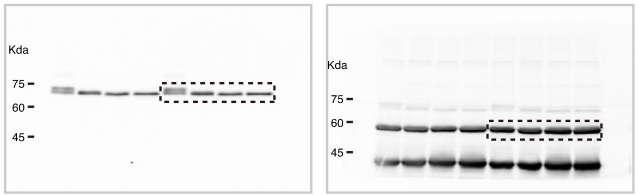

For Figure S7A

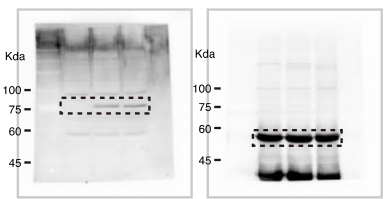

For Figure S7B

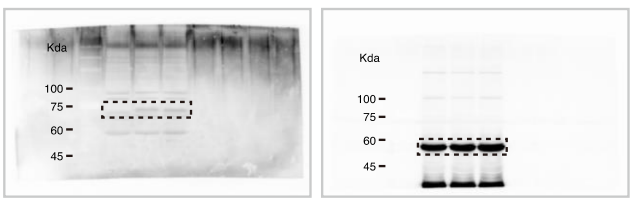

Fig. S9. Full images of Western blots.

Supplementary Table

Table S1. Yeast strains used in this study.

Strain	Genotype	Source
BY4741	*MATa his3Δ1 leu2Δ0 met15Δ0 ura3Δ0*	EUROSCARF
BY4742	*MATα his3Δ1 leu2Δ0 lys2Δ0 ura3Δ0*	EUROSCARF
HY1912	*MATa his3Δ1 leu2Δ0 met15Δ0 ura3Δ0 ura3::pGAL1-HO:URA3*	This study
HY1913	*MATa his3Δ1 leu2Δ0 met15Δ0 ura3Δ0 rad51Δ::kanMX4 ura3::pGAL1-HO:URA3*	This study
HY1914	*MATa his3Δ1 leu2Δ0 met15Δ0 ura3Δ0 rad52Δ::kanMX4 ura3::pGAL1-HO:URA3*	This study
HY1915	*MATa his3Δ1 leu2Δ0 met15Δ0 ura3Δ0 rad51Δ::kanMX4 his3::pADH1-GFP-RAD51:HIS3 ura3::pGAL1-HO:URA3*	This study
HY1916	*MATa his3Δ1 leu2Δ0 met15Δ0 ura3Δ0 rad52Δ::kanMX4 leu2::pADH1-RAD52-mCherry:LEU2 ura3::pGAL1-HO:URA3*	This study
HY1262	*MATa ade2-1 ura3-1 his3-11,15 trp1-1 leu2-3,112 can1-100 cdc28-as1*	Bishop et al. (2000)
HY1917	*MATa ade2-1 ura3-1 his3-11,15 trp1-1 leu2-3,112 can1-100 cdc28-as1-TAP:Leu2*	This study
TL16A05	*MATa his3Δ1 leu2Δ0 met15Δ0 ura3Δ0 CLN1-TAP:HIS3*	Ghaemmaghami et al. (2003)
TL16F05	*MATa his3Δ1 leu2Δ0 met15Δ0 ura3Δ0 CLN2-TAP:HIS3*	Ghaemmaghami et al. (2003)
TL14E08	*MATa his3Δ1 leu2Δ0 met15Δ0 ura3Δ0 CLN3-TAP:HIS3*	Ghaemmaghami et al. (2003)
TL20E04	*MATa his3Δ1 leu2Δ0 met15Δ0 ura3Δ0 CLB1-TAP:HIS3*	Ghaemmaghami et al. (2003)
TL19B03	*MATa his3Δ1 leu2Δ0 met15Δ0 ura3Δ0 CLB2-TAP:HIS3*	Ghaemmaghami et al. (2003)
TL23A06	*MATa his3Δ1 leu2Δ0 met15Δ0 ura3Δ0 CLB3-TAP:HIS3*	Ghaemmaghami et al. (2003)
TL21B02	*MATa his3Δ1 leu2Δ0 met15Δ0 ura3Δ0 CLB4-TAP:HIS3*	Ghaemmaghami et al. (2003)
TL22A11	*MATa his3Δ1 leu2Δ0 met15Δ0 ura3Δ0 CLB5-TAP:HIS3*	Ghaemmaghami et al. (2003)
TL26D06	*MATa his3Δ1 leu2Δ0 met15Δ0 ura3Δ0 CLB6-TAP:HIS3*	Ghaemmaghami et al. (2003)
HY1918	*MATa his3Δ1 leu2Δ0 met15Δ0 ura3Δ0 rad51Δ::kanMX4 his3::pADH1-GFP-RAD51(S125A, S375A):HIS3 ura3::pGAL1-HO:URA3*	This study
HY1919	*MATa his3Δ1 leu2Δ0 met15Δ0 ura3Δ0 rad51Δ::kanMX4 his3::pADH1-GFP-RAD51(S125E, S375E):HIS3 ura3::pGAL1-HO:URA3*	This study
HY1920	*MATa his3Δ1 leu2Δ0 met15Δ0 ura3Δ0 rad51Δ::kanMX4 his3::pADH1-GFP-RAD51:HIS3 ura3::pGAL1-HO:URA3 RAD52-myc:LEU2*	This study
HY1921	*MATa his3Δ1 leu2Δ0 met15Δ0 ura3Δ0 rad51Δ::kanMX4 his3::pADH1-GFP-RAD51(S125A, S375A):HIS3 ura3::pGAL1-HO:URA3 RAD52-myc:LEU2*	This study
HY1922	*MATa his3Δ1 leu2Δ0 met15Δ0 ura3Δ0 rad51Δ::kanMX4 his3::pADH1-HA-TEV site-RAD51:HIS3 ura3::pGAL1-HO:URA3*	This study
HY1923	*MATa his3Δ1 leu2Δ0 met15Δ0 ura3Δ0 rad51Δ::kanMX4 his3::pADH1-HA-TEV site-RAD51(S125A, S375A):HIS3 ura3::pGAL1-HO:URA3*	This study
HY1924	*MATa his3Δ1 leu2Δ0 met15Δ0 ura3Δ0 rad52Δ::kanMX4 leu2::pADH1-RAD52(T412A)-mCherry:LEU2 ura3::pGAL1-HO:URA3*	This study

HY1925	*MATa his3Δ1 leu2Δ0 met15Δ0 ura3Δ0 rad52Δ::kanMX4 leu2::pADH1-RAD52(T412E)-mCherry:LEU2 ura3::pGAL1-HO:URA3*	This study
HY1926	*MATa his3Δ1 leu2Δ0 met15Δ0 ura3Δ0 rad52Δ::kanMX4 leu2::pADH1-RAD52-mCherry:LEU2 ura3::pGAL1-HO:URA3 RFA1-GFP:HIS3*	This study
HY1927	*MATa his3Δ1 leu2Δ0 met15Δ0 ura3Δ0 rad52Δ::kanMX4 leu2::pADH1-RAD52(T412A)-mCherry:LEU2 ura3::pGAL1-HO:URA3 RFA1-GFP:HIS3*	This study
HY1928	*MATa his3Δ1 leu2Δ0 met15Δ0 ura3Δ0 rad52Δ::kanMX4 leu2::pADH1-RAD52(T412E)-mCherry:LEU2 ura3::pGAL1-HO:URA3 RFA1-GFP:HIS3*	This study
HY1929	*MATa his3Δ1 leu2Δ0 met15Δ0 ura3Δ0 rad52Δ::kanMX4 leu2::pADH1-RAD52-HA:LEU2*	This study
HY1930	*MATa his3Δ1 leu2Δ0 met15Δ0 ura3Δ0 rad52Δ::kanMX4 leu2::pADH1-RAD52(T412A)-HA:LEU2*	This study
HY1931	*MATa his3Δ1 leu2Δ0 met15Δ0 ura3Δ0 rad52Δ::kanMX4 leu2::pADH1-RAD52-TAP:LEU2 ura3::pGAL1-HO:URA3*	This study
HY1932	*MATa his3Δ1 leu2Δ0 met15Δ0 ura3Δ0 rad52Δ::kanMX4 leu2::pADH1-RAD52(T412A)-TAP:LEU2 ura3::pGAL1-HO:URA3*	This study
HY1933	*MATa his3Δ1 leu2Δ0 met15Δ0 ura3Δ0 rad52Δ::kanMX4 leu2::pRPL7B-VN-RAD52:LEU2*	This study
HY1934	*MATα his3Δ1 leu2Δ0 lys2Δ0 ura3Δ0 rad52Δ::URA3 leu2::pRPL7B-VC-RAD52:LEU2*	This study
HY1935	*MATa his3Δ1 leu2Δ0 met15Δ0 ura3Δ0 rad52Δ::kanMX4 leu2::pRPL7B-VN-RAD52(T412A):LEU2*	This study
HY1936	*MATα his3Δ1 leu2Δ0 lys2Δ0 ura3Δ0 rad52Δ::URA3 leu2::pRPL7B-VC-RAD52(T412A):LEU2*	This study
HY1937	*MATa his3Δ1 leu2Δ0 met15Δ0 ura3Δ0 rad52Δ::kanMX4 fpr1Δ::MET15 ura3::pGAL1-HO:URA3 his3::pCET1-RAD52-mCherry-FKBP:HIS3 leu2::pCET1-RAD52-GFP-FRB:LEU2*	This study
HY1938	*MATa his3Δ1 leu2Δ0 met15Δ0 ura3Δ0 rad52Δ::kanMX4 fpr1Δ::MET15 ura3::pGAL1-HO:URA3 his3::pCET1-RAD52(T412A)-mCherry-FKBP:HIS3 leu2::pCET1-RAD52(T412A)-GFP-FRB:LEU2*	This study
HY1939	*MATa his3Δ1 leu2Δ0 met15Δ0 ura3Δ0 rad52Δ::kanMX4 fpr1Δ::MET15 ura3::pGAL1-HO:URA3 his3::pADH1-RAD52(T412A)-mCherry:HIS3*	This study
HY2097	*MATa his3Δ1 leu2Δ0 met15Δ0 ura3Δ0 rad51Δ::kanMX4 PDS1-myc:LEU2 his3::pADH1-GFP-RAD51(S125A):HIS3*	This study
HY2098	*MATa his3Δ1 leu2Δ0 met15Δ0 ura3Δ0 rad51Δ::kanMX4 PDS1-myc:LEU2 his3::pADH1-GFP-RAD51(S375A):HIS3*	This study
HY2177	*MATa ade2-1 ura3-1 his3-11,15 trp1-1 leu2-3,112 can1-100 cdc28-as1 RAD52-HA:URA3*	This study
HY2178	*MATa his3Δ1 leu2Δ0 met15Δ0 ura3Δ0 RAD52-HA:URA3*	This study
HY2179	*MATa his3Δ1 leu2Δ0 met15Δ0 ura3Δ0 clb2Δ::kanMX4 RAD52-HA:URA3*	This study
HY2180	*MATa his3Δ1 leu2Δ0 met15Δ0 ura3Δ0 clb3Δ::kanMX4 RAD52-HA:URA3*	This study